

Noise-induced volatility of collective dynamicsGeorges Harras,¹ Claudio J. Tessone,² and Didier Sornette¹¹*Chair of Entrepreneurial Risks, D-MTEC, ETH Zurich, CH-8092 Zurich, Switzerland*²*Chair of Systems Design, D-MTEC, ETH Zurich, CH-8092 Zurich, Switzerland*

(Received 9 August 2011; revised manuscript received 10 October 2011; published 31 January 2012)

Noise-induced volatility refers to a phenomenon of increased level of fluctuations in the collective dynamics of bistable units in the presence of a rapidly varying external signal, and intermediate noise levels. The archetypical signature of this phenomenon is that—beyond the increase in the level of fluctuations—the response of the system becomes uncorrelated with the external driving force, making it different from stochastic resonance. Numerical simulations and an analytical theory of a stochastic dynamical version of the Ising model on regular and random networks demonstrate the ubiquity and robustness of this phenomenon, which is argued to be a possible cause of excess volatility in financial markets, of enhanced effective temperatures in a variety of out-of-equilibrium systems, and of strong selective responses of immune systems of complex biological organisms. Extensive numerical simulations are compared with a mean-field theory for different network topologies.

DOI: [10.1103/PhysRevE.85.011150](https://doi.org/10.1103/PhysRevE.85.011150)

PACS number(s): 05.40.–a, 89.65.–s

I. INTRODUCTION

Noise has effects *a priori* unexpected on the organization of complex systems made of interacting elements, as shown by *stochastic resonance* (SR) [1], *coherence resonance* [2], *noise-induced phase transitions* [3], noise-induced transport [4], and its game theoretical version, the *Parrondo's Paradox* [5]. SR occurs in a system when a small applied (subthreshold) periodic signal is amplified by the addition of noise and the maximum of amplification is found for intermediate noise strengths. More generally, SR refers to the situation where noise and nonlinearity combine to increase the strength in the system response. Among others, SR was shown to appear in optical [6] and magnetic systems [7,8], and was thought to be relevant in various fields, ranging from Earth climate [9] and the dynamics of ice ages [10], to neurobiology [11,12] and visual perception [13]. Generally SR is studied in bistable systems, where the amplification of a subthreshold periodic signal is achieved through the synchronization of noise-induced interwell hopping of the dynamic variable and the driving signal. The signal is maximally amplified when the level of noise is such that the Kramers time, which is the intrinsic lifetime associated with the noise-induced transition between the two stable states, equals half of the period of the external forcing. The bistability of the dynamic variable can be given either explicitly [14]—for low dimensional systems—or emerge from the interaction of the many constituents as for the magnetization in the Ising model in the ferromagnetic case [15,16]. However, systems of many interacting constituents may depart from the paradigmatic setting of SR, as there is no interwell hopping for the macroscopic observable, and thus the bistability is only preserved at the microscopic level.

The Ising model, driven by a periodic signal, has been extensively studied in the realm of the kinetic Ising model and dynamical phase transitions [15–20]. When a spatially extended Ising system—for temperatures below the Curie temperature—is forced by a weak periodic influence, the magnetization performs dynamics around its nonzero equilibrium fixed point, resulting in a nonzero time-averaged magnetization. For a given temperature, by increasing either the field strength or the period of the signal, the system becomes able to hop between the two symmetric equilibrium fixed points

inducing a zero average magnetization. The nature of this transition, from a nonzero to a zero average magnetization, can be manifold and depends on the control parameter. For weak, subthreshold forcing strength and finite-size systems—where interwell hopping is enabled by the fluctuations—SR is at the origin of the transition. In large enough systems, such that finite-size fluctuations can be neglected, and for intermediate field strengths, they experience a dynamical phase transition through a nucleation process [16]. For stronger forcing, the transition is forced by the exogenous field, with no contribution from endogenous factors.

In this paper, we investigate the behavior of systems composed of many interacting constituents under the influence of a time-varying external forcing. The Ising model framework is used as a generic example of such systems. In contrast to the classical SR studies, where the period of the periodic forcing is of the order of the Kramers time, we are interested in much faster signals. Additionally, aperiodic signals are included to the external forcing, a setup much closer to real world examples, which will yield some surprising differences to the cases involving periodic forcing.

We find, for periodic and aperiodic signals alike, that for intermediate values of the noise intensity, the system dynamics shows a maximum in amplitude [8,21]. Interestingly, the phenomenon of increased amplitude, which consists of an amplification of the signal for a periodic forcing, morphs into an increase of the system-wide fluctuations, uncorrelated with the signal for an aperiodic forcing. We call this phenomenon “*noise-induced volatility*” (NIV).

There are many examples of systems composed of a large number of interacting units that are subjected to a rapidly varying—periodic or aperiodic—common forcing. A first example refers to the empirical observations of strong amplifications of thermal noise into effective renormalized temperatures by quenched heterogeneities in materials [22], in organized flows in liquids [23] and in granular media near jamming [24]. We argue that NIV also provides a conceptual framework to model the immune systems of complex biological organisms, viewed as multistable complexes, which switch their mode of operation under the influence of noisy perturbations by pathogens and other stress factors [25–27].

Another important application of the proposed mechanism of volatility amplification can be found in financial markets. The phenomenon of “excess volatility” [28] constitutes one of the major unsolved puzzles in financial economics and refers to the ubiquitous observation that financial prices fluctuate with much larger amplitudes than they should if they obeyed the fundamental valuation formula, linking the share price of a company to its expected future dividends and discount factors [29]. The model described below can be applied to represent a market of interacting investors, where the external forcing represents the news (i.e., the publicly available information about the traded assets) that investors use to update their estimates of the asset’s fair value. In addition to the phenomenon of the increased volatility compared to the news amplitude, our framework allows us to address two other well-known phenomena of financial markets: namely, the fact that the news is a poor predictor of future price changes [30] and the phenomenon of clustered volatility, quantified by the slowly decaying temporal dependence of volatility [31].

We document the phenomenon of noise-induced volatility by numerical and theoretical calculations on a stochastic dynamical version of the Ising model on fully connected, regular as well as random networks, in the presence of rapidly varying periodic and aperiodic signal. NIV also constitutes a new indicator for an approaching phase transition [32].

This paper is organized as follows. In the following section, we introduce the model studied and the measures chosen to quantify the phenomenon studied. In Sec. III, we revisit the case where the system is driven by a periodic forcing, focusing on the case of fast signals, by means of Monte Carlo simulations and by means of an analytical approach. In Sec. IV, we present the main contribution of the paper: the study of the system driven by an aperiodic forcing. In Sec. V, we go beyond the fully connected case, focusing on different network topologies and on a paradigmatic example of this phenomenon: the excess volatility in financial markets. Finally, Sec. VI presents a discussion and conclusions of the obtained results.

II. MODEL DESCRIPTION AND DIAGNOSTIC VARIABLES

Consider a system composed of N interacting units that can be in one of two states: $s = \pm 1$. The units are updated sequentially, randomly chosen at each unit micro-time $\delta = 1/N$ (i.e., N updates are equivalent to one time unit at the macroscopic level, that is, one Monte Carlo step [33–35]). The update of the state s_i of a given unit i from t to $t + \delta$ is given by

$$s_i(t + \delta) = \text{sgn} \left(f(t) + \xi_i(t) + K(t) \sum_{j=1}^N \omega_{ij} s_j(t) \right). \quad (1)$$

The value $s_i(t + \delta)$ is determined by three competing contributions: (i) a common external dynamic forcing term $f(t)$ (force, pathogens abundance, news); (ii) an annealed unit-specific term $\xi_i(t)$ that we will call *noise* (thermal fluctuations or threshold, intrinsic susceptibility of a unit immune system compartment, investor idiosyncratic opinion, or private information); (iii) an interaction term between units controlled by

the amplitude $K(t)$ (elastic coupling, feedback loops between immune system elements, social impact).

The system’s behavior will be investigated under the influence of two different types of external signals. To relate to the existing literature, we will use a smooth periodic signal, $f_p(t) = A \sin(\omega t)$, with period $2\pi/\omega$ and strength A ; this implies that, when averaged over time, the standard deviation of the signal is $\sigma_{f_p} = A/\sqrt{2}$. Along this paper, we denote by *signal amplitude* the standard deviation of the signal σ_f . As a periodic signal is a rather stylized and artificial setup, we will, in a later section, also analyze the response of such a system to a stochastic process. The simplest choice of a stochastic process with tunable characteristic time scale is the Ornstein-Uhlenbeck (OU) process, which has exponentially decaying memory and is defined by $df_{ap} = -\theta f_{ap} dt + A dW_t$, with 0 mean, strength A , inverse time scale $\theta > 0$ and W_t is a Wiener process with normalized variance and zero mean. The asymptotic solution of the OU process is

$$f_{ap}(t) = A \int_{-\infty}^t e^{-\theta(t-\tau)} dW_\tau, \quad (2)$$

which gives a signal amplitude $\sigma_{f_{ap}} = A/\sqrt{2\theta}$.

The noise term $\xi_i(t)$ of each unit in Eq. (1) follows an independent stochastic process, whose values are, at every micro-time-step, drawn from the cumulative distribution function $G(0, D)$, with zero mean ($\langle \xi_i(t) \rangle = 0$) and variance D^2 . Thus, $\langle \xi_i(t) \xi_j(t + n\delta) \rangle = D^2 \delta_n \delta_{ij}$. If $f(t) = 0$ and $G(0, d)$ corresponds to a logistic distribution, the dynamical rule of Eq. (1) is equivalent to the kinetic Ising model with Glauber dynamics (cf. appendix) where D^2 is related to the temperature.

In the interaction term in Eq. (1), the matrix of weights ω_{ij} defines the network connectivity between units, both in topology and relative strength. We assume that the interactions between units are governed by connections that evolve much slower than the dynamics of the whole system. This amounts to considering a static network with fixed normalized weights $\sum_j \omega_{ij} = 1$. The effective coupling strength is given by $K(t)$, which may depend on time to reflect global softening-hardening in rupture processes, evolving physiological states of immune systems, and changes of social cohesiveness and/or social influence in financial markets.

The macroscopic dynamics of the system is captured by the instantaneous “magnetization”:

$$m(t) = \frac{1}{N} \sum_i s_i(t), \quad (3)$$

which fluctuates around its time-average Q , which is computed as

$$Q = \langle m(t) \rangle_t = \frac{1}{T} \int_0^T m(t) dt, \quad (4)$$

where T is the duration of the simulation. We study the normalized standard deviation:

$$\tilde{\sigma} = \frac{\sigma_m}{\sigma_f} = \frac{\sqrt{\langle [m(t) - Q]^2 \rangle_t}}{\sqrt{\langle f(t)^2 \rangle_t}}, \quad (5)$$

of $m(t)$, describing the “volatility” of the system dynamics scaled by the signal amplitude, σ_f . As the response of

the system to an external influence is not instantaneous, the time-lagged correlation between the input signal and the magnetization, defined by

$$\rho(\tau) = \frac{\langle [m(t + \tau) - Q]f(t) \rangle_t}{\sigma_m \sigma_f}, \quad (6)$$

provides an additional insight on the level of synchronization between the external influence and the overall system dynamics at a lag of τ . The lag where the correlation is maximal will be called optimal lag, $\tau^* = \max_{\tau} \rho(\tau)$.

In the case of the periodic signal, a common measure in stochastic resonance research is the spectral amplification factor (SAF) [36],

$$R = \frac{S_{\omega}[m(t)]}{S_{\omega}[f_p(t)]} = \frac{S_{\omega}[m(t)]}{\sigma_f^2}, \quad (7)$$

which is the ratio of the power spectrum density of the magnetization $S_{\omega}[m(t)]$ over the power spectrum density of the driving signal, $S_{\omega}[f_p(t)] = \sigma_f^2 = A^2/4$, both at the driving frequency ω .

III. PERIODIC SIGNAL

A. Simulations results

First, we consider an homogeneous, complete, network ($\omega_{ij} = 1/(N - 1)$) and a constant coupling strength $K(t) = k = 1$. The results reported below are not significantly different for random graphs with large average connectivity or when the connections allow for an unbiased statistical sampling within the population. As previously said, we set G to be a Gaussian distribution with standard deviation D , and zero mean. Even though the system loses its equivalence to the kinetic Ising model with Glauber dynamics, all the qualitative properties of the system remain unchanged. Without external forcing ($A = 0$), the system experiences, as for the equilibrium Ising model, a continuous phase transition at $D_c \simeq 0.80k$, separating the ordered phase with two stable fixed points at $\pm Q(D)$, from the disordered phase, with a single stable fixed point at $Q(D) = 0$. For the equilibrium case ($A = 0$), the dependence of $Q(D)$ as a function of D is shown by the continuous line in Fig. 1(b).

In Fig. 1(a), we plot the spectral amplification factor as a function of noise strength for signals with different periods. The symbols are obtained by simulations of the model with 10^6 units. We observe that, even for relatively small periods, an increase of amplification exceeding one order of magnitude is achieved for a broad range of intermediate value of noise, the hallmark of stochastic resonance. Figure 1(b) shows the average magnetization, $Q(D)$, which is the usual order parameter in the kinetic Ising model studies, for the same signals as in Fig. 1(a). In Sec. III B, we will develop a theory which shows that the global dynamics can be assimilated to a motion within a potential that exhibits a transition from a monostable to a bistable regime. For fast signals, $Q(D)$ has a value close to the equilibrium fixed point (continuous line), suggesting that the dynamics of $m(t)$ can be well described as fluctuations around this stable (or metastable) point, i.e., $m(t)$ performs intrawell dynamics. For slower signals, larger fluctuations around the equilibrium fixed point are observed,

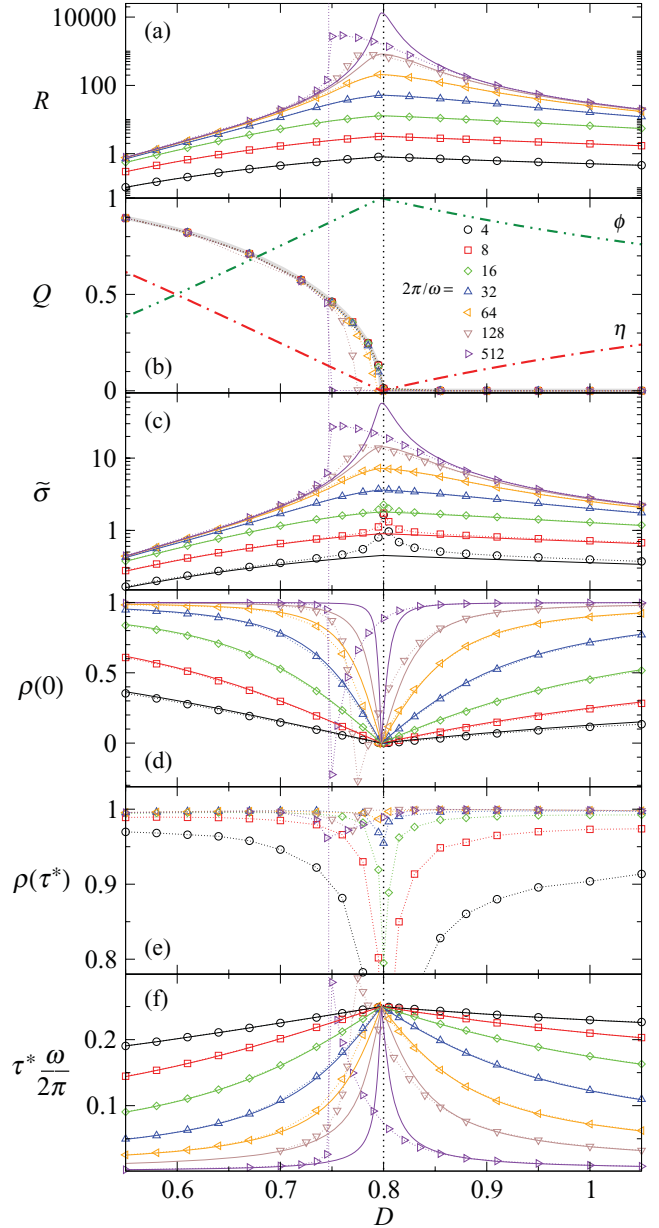


FIG. 1. (Color online) (For periodic signals) Different measures as a function of the standard deviation of the noise in Eq. (1), D , for weak periodic signals with amplitude $\sigma_{fp} = 0.01$. The period of the signal is in the legend of (b). Symbols are obtained for simulations with a system size $N = 10^6$ and the lines are the result of the linear approximation presented in the main text. The vertical thin dotted line indicates D_T for $\omega = 2\pi/512$, where the transition from intra- to interwell dynamics occurs. The vertical thick dotted line indicates the critical value of noise D_c , where the phase transition takes place. For $D \in]D_T, D_c[$, $m(t)$ performs interwell dynamics. (a) Spectral amplification factor R , as defined by Eq. (7). (b) Average magnetization Q . For $D < D_c$, $Q = 0$ indicates that the system performs interwell dynamics. (c) The normalized standard deviation, $\tilde{\sigma}_p$. (d) Instantaneous correlation between m and f , $\rho(0)$, defined by Eq. (6). (e) Correlation between m and f at the optimal lag. (f) Optimal lag, τ^* , normalized by the period of the driving force.

as $Q(D)$ vanishes already for $D < D_c$, indicating symmetric oscillations around $m(t) = 0$, i.e., $m(t)$ performs interwell

dynamics. By $D_T(A, \omega, N)$, we denote the threshold value of the noise strength at which the potential barrier between the two equilibrium fixed points become small enough, such that the system performs interwell hopping and thus $Q(D)$ goes to zero. The noise strength threshold D_T approaches D_c as either ω or N are increased or A is decreased. In the opposite limits, it will tend to zero.

Independent on the driving frequency, the maximum in the amplification is always found at D_T . For fast signals where $D_T \sim D_c$, this maximum is observed at the equilibrium phase transition. This happens in the presence of two competing phenomena near the equilibrium phase transition: on the one hand, a divergence in the susceptibility, making the system very sensitive to small changes in the external influences; on the other, critical slowing down, which inhibits the reaction of the system. For slow signals, where $D_T < D_c$, together with a more abrupt vanishing of Q , a pronounced jump in the spectral amplification factor R , defined in Eq. (7), is observed at $D = D_T$, where the response of the system is greatly increased by the transition from intra- to interwell dynamics. For $D_T < D < D_c$, the amplification decreases with D , as the position of the minimum ($\pm m_0(D)$) approaches 0 for D approaching D_c from the left.

Figure 1(d) shows the dependence of the correlation at zero lag on the noise strength. A minimum of instantaneous correlation is observed at the same values of D , where the maximum in R occurs. This result confirms the existence of a double peak of the non-normalized instantaneous covariance, as was found by Leung *et al.* [7,8].

The effect of the signal frequency on the system behavior is shown in Fig. 2, where we plot the amplification R as a function of the period of the signal for different values of D . For

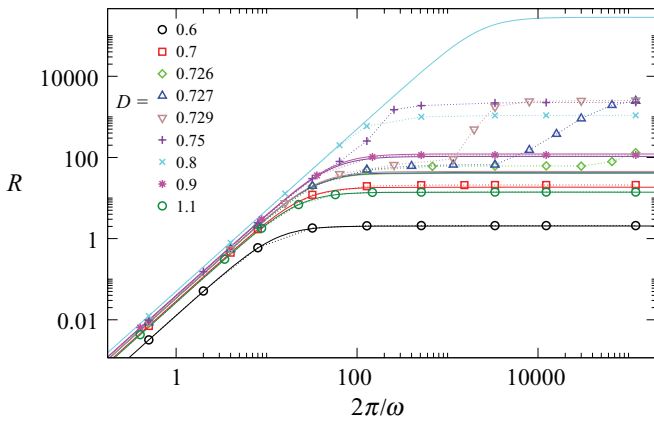


FIG. 2. (Color online) For periodic signals with amplitude $\sigma_{fp} = 0.02/\sqrt{2}$ and different values for the standard deviation of the noise D specified in the legend. The spectral amplification factor R as a function of the period, $2\pi/\omega$. Symbols are obtained for simulations of a system with $N = 9 \times 10^4$ and the lines represent the linear approximation given by Eq. (15). Three regimes of R can be identified as a function of the period: (1) increasing amplification with increasing period, (2) plateau with intrawell dynamics, (3) for $D \lesssim D_c$, stark increase of amplification due to interwell dynamics. Similar results are found for larger system sizes, where the third regime appears for larger periods as the finite-size fluctuations are reduced.

$D > D_c$, where the macroscopic system dynamics is described by a monostable potential, the dependence is composed of two regimes. The first regime is where the amplitude of the oscillations of $m(t)$ increases with the period as $m(t)$ is pushed for longer durations into one direction, allowing for greater deviations from the origin. For larger signal periods, R reaches a plateau, which constitutes the second regime, where the diffusive motion of $m(t)$ is confined by the potential. The same behavior is observed for $D \ll D_c$, where the potential barrier between the two minima cannot be overcome by the system, restricting the dynamics to intrawell motions. Finally, for $D \lesssim D_c$, the dependence shows a transition into a third regime. If the potential barrier is not too high compared with the noise intensity and the finite-size fluctuations, the system is able to perform interwell dynamics for large enough periods of the external driving. These interwell dynamics are observed as a second rapid increase in R . The period at which this transition happens is the double of the Kramers time.

B. Analytical approach

In order to understand these results, we now develop a mean-field theory, which becomes exact in the thermodynamic limit and for weak signal amplitudes. As our system is composed of many interconnected units, we can rewrite Eq. (1) by replacing the interaction term by the global instantaneous magnetization and by explicitly writing down Eq. (1) in the form of

$$s_i(t + \delta) = \begin{cases} +1 & \text{if } \xi_i(t) \geq -k m(t) - f(t) \\ -1 & \text{if } \xi_i(t) < -k m(t) - f(t) \end{cases}$$

Averaging over multiple noise realizations, the expected value for the state of the i th unit, at time $t + \delta$ is thus given by

$$\begin{aligned} \langle s_i(t + \delta) \rangle_\xi &= 1 - G(-k m(t) - f(t)) - G(-k m(t) - f(t)) \\ &= 1 - 2G(-k m(t) - f(t)), \end{aligned} \quad (8)$$

where $G(\theta)$ is the cumulative distribution function of the noise term $\xi_i(t)$, i.e., $G(\theta) = \int_{-\infty}^{\theta} d\theta' g(\theta')$. Summing over all the units and given that only spin i is updated over the micro-time-step δ , we get that the updated instantaneous magnetization is exactly

$$m(t + \delta) = m(t) + \frac{1}{N} [s_i(t + \delta) - s_i(t)]. \quad (9)$$

By averaging over the complete population and identifying $1/N \delta$ as dt in the thermodynamic limit, Eq. (9) transforms into a continuous process, which reads

$$\left\langle \frac{dm(t)}{dt} \right\rangle = \langle s_i(t + dt) \rangle - m(t). \quad (10)$$

With $\dot{m}(t) = \langle dm(t)/dt \rangle$ and substituting Eq. (8) into Eq. (10), we get

$$\dot{m}(t) = -m(t) + 1 - 2G(-k m(t) - f(t)), \quad (11)$$

which constitutes a general closed form evolution equation for the magnetization of the system.

From the point of view of the mean-field limit, the noise $\xi_i(t)$ can be either quenched or annealed, as the complete noise is condensed into the last term in Eq. (11). For $A = 0$ (no external driving), the stationary solution of Eq. (11) gives

the dependence of the equilibrium fixed point $m_0(D)$ as the solution of the implicit equation,

$$m_0(D) = 1 - 2G(-km_0(D)). \quad (12)$$

This solution exhibits a supercritical pitchfork bifurcation as a function of D , as expected for an Ising-like system, which is displayed by the continuous line in Fig. 1(b). The critical parameter is found equal to $D_c = k\sqrt{2/\pi}$, when $\xi_i(t)$ is drawn from a Gaussian distribution.

The emphasis of this paper is on the system's reaction to fast, subthreshold ($A \ll 1$) signals, so that interwell dynamics can be neglected. Thus, a perturbation expansion $m(t) = m_0 + m_1(t)$ up to first order yields

$$\frac{d}{dt}m_1(t) = -\eta(D)m_1(t) + \phi(D)f(t) + O(m_1^2), \quad (13)$$

where $\phi(D) \equiv 2g(-km_0)$, $\eta(D) \equiv 1 - 2kg(-km_0)$, and $g = dG/d\xi$. The dependence of ϕ and η as a function of the noise strength is displayed by the dash-dotted lines in Fig. 1(b). Based on Eq. (13), $\phi(D)$ can be interpreted as the attenuation of the signal by the noise in the individual constituents of the system as $\phi(D) \leq 1/k$ for any D . The value of $\phi(D)$ weights the impact of the external forcing on the global dynamics. The parameter $\eta(D)$ can be understood as the strength of the restoring force that tends to bring $m(t)$ back to its equilibrium value m_0 , after being driven away by the influence of $f(t)$. The larger η , the closer the dynamics of $m(t)$ will be to m_0 and the shorter will be the memory of $m(t)$. The value of $\eta(D)$ controls the contribution of the endogenous part of the dynamics. In the particular case where $f(t)$ is constant, $m_1(t)$ approaches the fixed point $f\phi(D)/\eta(D)$. Since $\phi(D)$ remains finite when D passes through D_c , it is the vanishing of $\eta(D)$ at $D = D_c$ and its smallness in the vicinity of D_c that is at the origin of the amplified volatility. Based on Eq. (13), we can now compute the approximate value of the different measures for the external signals and compare them to the simulations of the actual system.

For the periodic forcing, the dynamics of the magnetization yields

$$m_p(t) = \frac{A\phi}{\eta^2 + \omega^2}[-\omega \cos(\omega t) + \eta \sin(\omega t)] + m_0. \quad (14)$$

Together with Eq. (7), this gives a spectral amplification factor equal to

$$R_p = \frac{4}{A^2} \left(\frac{A\phi}{\eta^2 + \omega^2} \right)^2 \frac{\omega^2 + \eta^2}{4} = \frac{\phi^2}{\eta^2 + \omega^2}. \quad (15)$$

Figure 1(a) shows that, for fast signals (where $D_T \simeq D_c$), the value of R obtained from this approximation matches well with the simulation results. Deviations from the approximation appear for slower signals when D_T does not coincide with D_c and nonlinear effects cannot be neglected anymore.

As can be seen in Fig. 1(a), the spectral amplification factor can reach values above 100, showing that this system, even without considering interwell dynamics, is able to show remarkable reactions to a weak forcing. Two distinct amplification mechanisms of subthreshold periodic signals can be identified by comparing the simulation with approximation results. The first mechanism, being present for finite and infinite systems, is the increase of the output amplitude by

the decrease of the value of η : By reducing the restoring force of $m(t)$, such that it can be further displaced from m_0 , the oscillation amplitudes are increased. The second mechanism is the amplification through interwell jumps, which is only present in finite systems, as a subthreshold driving force cannot overcome the potential barrier without the existence of a source of fluctuations, like finite-size effects. Note that in the thermodynamical limit, where the approximation is valid for any frequency, at D_c where $\eta(D_c) = 0$, it follows from Eq. (15) that the fluctuations of $m(t)$ for nonzero frequencies will always be finite.

In addition to the spectral amplification factor R , we also measure the normalized variance of $m(t)$, $\tilde{\sigma}$, which measures the volatility of the dynamics, independent of the exact shape of the power spectrum. This measure is convenient as it can be used for comparison with the aperiodic signal, for which R is not defined. From Eq. (14), the normalized variance of $r(t)$ is

$$\tilde{\sigma}_p^2 = \frac{2}{A^2} \langle m_p(t)^2 \rangle_t = \frac{2}{A^2} \frac{\omega}{2\pi} \int_0^{\frac{2\pi}{\omega}} m_p(t)^2 dt = \frac{\phi^2}{\eta^2 + \omega^2}. \quad (16)$$

The equivalence between Eqs. (15) and (16) is due to the use of a linear response approximation in the macroscopic dynamics of the systems, neglecting the response at higher order harmonics of the driving signal. As a consequence, the approximation of the spectral amplification factor R_p is better fitted by the simulations than $\tilde{\sigma}_p$.

From Fig. 1(c), we see that the mean-field approximation matches well the values of $\tilde{\sigma}$ obtained by simulations for intermediate signal periods. For large periods, the interwell dynamics destroys the match, and for fast signals (small periods), the finite-size fluctuations overshadow the fluctuations induced by the signals.

The correlation between $m_p(t)$ and $f_p(t)$ is given by

$$\rho_p(\tau) = \frac{\eta \cos(\omega\tau) + \omega \sin(\omega\tau)}{\sqrt{\eta^2 + \omega^2}}, \quad (17)$$

and, for the optimal lag, we obtain

$$\tau_p^* = \frac{\arctan(\frac{\omega}{\eta})}{\omega}, \quad (18)$$

which follows directly from Eq. (14). The correlation at zero lag is shown in Fig. 1(d). As for the results of R , the simulation results are well captured by the mean-field approximation for high frequencies and deviate due to interwell dynamics for lower frequencies. As was observed in [8], a dip in correlation is observed for intermediate values of the noise amplitude. This dip occurs at D_T , concomitant with the maximum in the amplification measured by R . This apparent contradiction can be explained by the results shown in Fig. 1(f), which plots the optimal lag between $m(t)$ and $f(t)$ normalized by the period of the signal. At D_T , $m(t)$ and $f(t)$ are maximally lagged, reducing the correlation at lag zero. On the other hand, the correlation at the optimal lag has a value close to one, explaining the high amplification of the signal. This behavior can also be found in the approximation, although there the maximum of amplification and minimum of instantaneous correlation is found at D_c as our approximation neglects interwell dynamics. From Eqs. (17) and (18) it follows that,

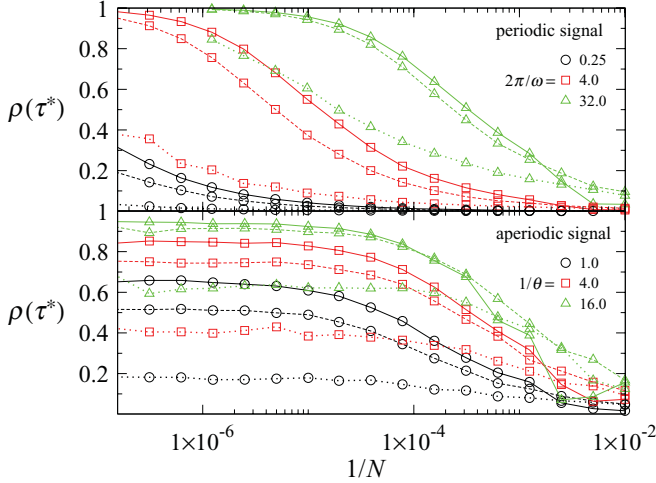


FIG. 3. (Color online) Size dependence of the maximal correlation between the magnetization and the signal with $\sigma_f = 0.01$ and different time scales for several noise intensities: $D = 0.7$ (solid lines), $D = 0.8$ (dotted lines), $D = 0.9$ (dashed lines). Characteristic time scales of the signal are specified in the legends. (top) Periodic signals, where $\rho(\tau^*)$ converges to 1 for any value of D in the thermodynamic limit. The rate of convergence increases with the signal period. (bottom) In case of aperiodic signals, the value of $\rho(\tau^*)$ does not converge to 1 in the thermodynamic limit and depends on D and θ . At $D = D_c$, the maximal correlation $\rho(\tau^*)$ is significantly reduced compared to $D \neq D_c$.

in the thermodynamic limit, there exists an optimal lag τ_p^* , for which perfect correlation is achieved for any frequency and any noise strength, i.e., $\rho_p(\tau_p^*) = 1$.

However, perfect correlation is not achieved for any frequency in finite systems as shown by the dependence of $\rho(\tau^*)$ in Fig. 1(e), where the deterioration of the correlation with increasing driving frequencies is observed. The origin of this effect lies in the finite-size fluctuations, which vanish in the thermodynamic limit, as Fig. 3 (top) shows. $\rho(\tau^*)$ converges to 1 for infinite systems, at a rate of convergence depending on D and the driving period.

IV. APERIODIC SIGNAL

We now turn our attention to the case where the common forcing is aperiodic. In this section, we will consider an external force, which is described by the OU process introduced in Eq. (2). Figure 4 illustrates the typical dynamic behaviors of $m(t)$ for different values of noise strengths D for a single realization of the driving force $f_p(t)$. For $D \geq D_c$, the magnetization fluctuates around $m_o(D) = 0$, with increasing amplitudes as D approaches D_c . The fluctuation amplitude decreases again when $m(t)$ performs intrawell dynamics for $D < D_c$, where $Q(D) \neq 0$.

We will compute the same observables as for the periodic signal and investigate the differences. The formal solution of the linearized version of the dynamics, Eq. (13), is given by

$$m_1(t) = A \phi \int_{-\infty}^t e^{-\eta(t-\tau)} \int_{-\infty}^{\tau} e^{-\theta(\tau-\tau')} dW_{\tau'} d\tau, \quad (19)$$

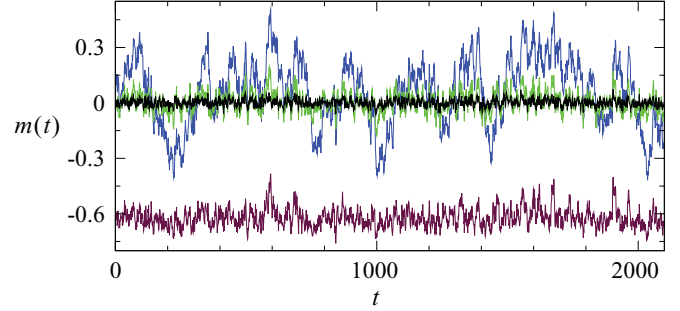


FIG. 4. (Color online) For aperiodic signals: time evolution of the magnetization $m(t)$ for different noise intensities D obtained with the same realization of the driving force $f(t)$ and $\xi_i(t)$. $N = 10^4$, $\sigma_{ap} = 0.04$, $\theta = 1.0$, $k = 1.0$, $D = 2.0, 1.0, 0.8$ (smaller to larger amplitude of $m(t)$'s fluctuations), and $D = 0.7$ (bottom curve fluctuating around $m(t) = -0.6$).

which describes the dynamics around m_0 . The normalized variance of $m_1(t)$ described by Eq. (19) is now given by

$$\tilde{\sigma}_{ap}^2 = \frac{\phi^2}{\eta(\theta + \eta)}. \quad (20)$$

In Fig. 5(a), we compare the normalized variance obtained by means of numerical simulations with this theoretical result. We find a very good agreement between the two for fast signals, with the same deficits due to inter-well dynamics as for the periodic case with slower signals. However, by comparing $\tilde{\sigma}_{ap}$ for the aperiodic signal with the periodic case $\tilde{\sigma}_p$, we observe a major difference. Whereas for the periodic case, the volatility of the dynamics shows a finite maximum value at D_c , the volatility diverges if the system is driven by an aperiodic signal as $\eta(D_c) = 0$. This divergence of the normalized volatility $\tilde{\sigma}_{ap}$ is not to be understood as an explosion of the dynamics, as $m(t)$ cannot exceed $[-1, +1]$. It reflects the immensely amplified reaction to a weak external forcing, consistent with the diverging susceptibility in equilibrium phase transitions. The fact that this divergence is absent for a periodic forcing stems from the discreteness of the power spectrum of the input signal. It is worth mentioning that the good match between the analytical approach—which becomes exact in the thermodynamic limit—and the numerical simulations shows that the phenomenon is not due to finite-size fluctuations, but is an emergent property of the system.

The correlation between the forcing $f_{ap}(t)$ and the magnetization, $m(t + \tau)$, is given by

$$\rho_{ap}(\tau) = \frac{\sqrt{\eta^2 + \theta\eta}}{\eta^2 - \theta^2} [(\eta + \theta)e^{-\theta\tau} - 2\theta e^{-\eta\tau}] \quad (21)$$

and is shown in Fig. 5(b) for zero lag, together with the simulation results, which are found in good agreement. The optimal lag for which $\rho_{ap}(\tau)$ is maximum occurs at

$$\tau_{ap}^* = \frac{\ln\left(\frac{\eta+\theta}{2\eta}\right)}{\theta - \eta}, \quad (22)$$

yielding a maximal correlation of

$$\rho_{ap}(\tau_{ap}^*) = 2^{\frac{\theta}{\theta-\eta}} \left(\frac{\eta}{\theta + \eta} \right)^{\frac{\eta+\theta}{2(\theta-\eta)}}. \quad (23)$$

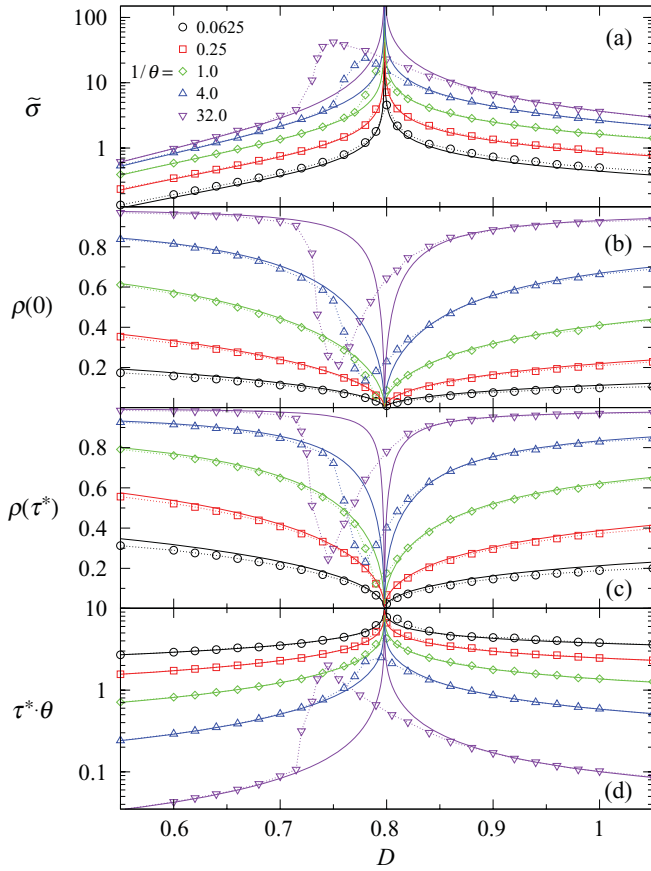


FIG. 5. (Color online) For aperiodic signals: different measures as a function of the standard deviation of the noise in Eq. (1), D , for weak aperiodic signals with amplitude $\sigma_{fp} = 0.01$. The inverse of the signal's time scale θ is given in the legend. Symbols are obtained for simulations with a system size $N = 10^6$ and the lines are the result of the linear approximation presented in the main text. (a) Normalized standard deviation $\tilde{\sigma}$, measuring the volatility amplification. (b) Instantaneous correlation between m and f , $\rho(0)$, defined by Eq. (6). (c) Correlation between m and f at the optimal lag. In contrast to the periodic signal, a system driven by an aperiodic signal is not able to follow the signal, even at the optimal lag, which is well described by the mean-field approximation. (d) Optimal lag τ^* normalized by the time scale of the signal.

Here, we find the second major difference between the periodic and aperiodic driving. For the periodic signal, it is always possible to find a lag at which the correlation between the forcing and the system's response is perfect. For the aperiodic signal (see Figs. 5(c) and 3 (bottom)), on the other hand, even in the thermodynamic limit, the dynamics of the system can be almost unrelated to the forcing. Perfect correlation is only reachable for very slow signals, i.e., $\lim_{\theta \rightarrow \infty} \rho_{ap}(\tau_{ap}^*) = 1$. Given that the forcing—an OU process—has a continuous power spectrum, and that the response of the system is frequency dependent, the spectrum of the macroscopic dynamics is distorted when compared to the one of the forcing, which has the effect of decreasing the correlation. Indeed, the system is only able to follow the part of the signal spectrum with frequencies lower than $\eta(D)$, which describes the rate at which the system can effectively react to external stimuli. As with decreasing θ , the contribution of lower frequencies

in the signal's spectrum is higher, the correlation for fixed D increases with decreasing θ .

For $D \approx D_c$, the volatility amplifies many times that of the driving signal $f(t)$. Concomitantly, ρ vanishes for every value of the lag τ , indicating that the volatility of the system is generated by an internal collective behavior. It is important to note that, even though the system dynamics are endogenously generated, they are initiated by an exogenous driving of the system. This is further confirmed by the good agreement between the approximation and simulations for fast signals. It is the shadow of the diverging susceptibility together with the vanishing rate of the reaction of the equilibrium model at D_c , which is responsible for the observed NIV phenomenon.

V. EXTENSIONS OF THE PHENOMENON STUDIED

A. Different networks

To show that the NIV phenomenon, characterized by the increase of volatility and decrease of correlation to the aperiodic forcing, is robust with respect to the structure of the network, Fig. 6 shows the normalized volatility $\tilde{\sigma}$ and the maximum in correlation $\rho(\tau^*)$ as a function of D (the standard deviation of the noise term in Eq. (1)) for different networks. We consider a two-dimensional regular grid with Moore neighborhood and random small-world connections with varying concentration p_w . Changing p_w from 0 to 1 interpolates between the regular two-dimensional (2D) lattice and the completely random network. For each p_w , the peak in volatility is still concomitant with the vanishing of ρ at the threshold value $D_T(p_w)$. The noise intensity threshold $D_T(p_w)$ is increasing in p_w , as larger global interconnection enhances the cooperative organization, and larger noise is needed to destroy the ferromagnetic state.

For one-dimensional (1D) lattices, the NIV phenomenon is still present, with a minimum in the cross correlation and a maximum in the volatility at D_T . As is well known, the

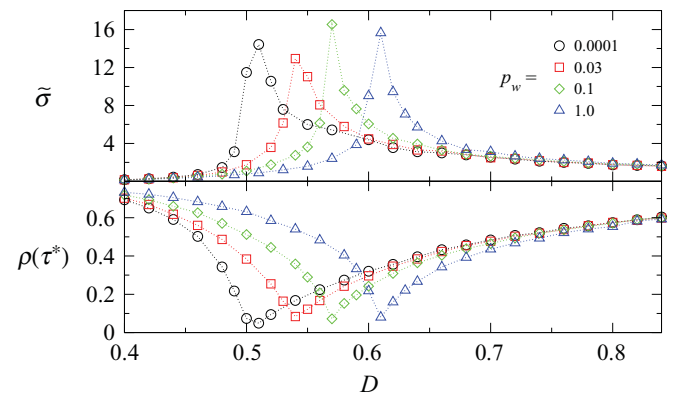


FIG. 6. (Color online) For an aperiodic signal: (top) the normalized volatility $\tilde{\sigma}$ and (bottom) the correlation at optimal lag $\rho(\tau^*)$ as a function of the standard deviation of the noise D for different small-world random connection concentrations p_w of a two-dimensional regular grid with Moore neighborhood. For $p_w = 0$, the network is a 2D regular grid with Moore neighborhood. For $p_w = 1.0$, the network is a random graph with an average degree, $d = 4$. The other system parameters are $N = 10^6$, $\sigma_f = 0.01$, $\theta = 1$, $k = 1$.

one-dimensional Ising model undergoes a first-order phase transition at zero temperature, and D_T converges to 0 in the thermodynamic limit. Notwithstanding the absence of a continuous phase transition, the susceptibility and relaxation time still diverge, exhibiting an essential singularity at zero temperature [37,38], which explains the survival of the NIV phenomenon in 1D.

B. Excess volatility in financial markets

By the definition of our model given by Eq. (1), it is clear that it is also interpretable as a model of opinion dynamics, where $s_i(t)$ is the opinion of agent i at time t , in line with the established literature on discrete choice [39]. The external forcing $f(t)$ can be seen as the flux of news, which is common to all agents, the noise $\epsilon_i(t)$ contains the agents' private information and the coupling term represents the social interaction between agents. The dynamics of the global opinion is then given by $m(t)$.

When applied to the social system of financial markets, the agents are investors and $s_i(t)$ corresponds to their opinion on whether the asset is over- or underpriced and hence to their willingness to buy (+1) or to sell (-1). The global demand is the given by $m(t)$, which impacts on the price as

$$\log[p(t+1)] = \log[p(t)] + \frac{m(t+1)}{\lambda}. \quad (24)$$

Here λ represents the liquidity depth of the market, which is assumed constant and $m(t)/\lambda$ is the financial return $r(t)$ from period t to period $t+1$. This equation expresses a linear market impact of the demands, which is a common hypothesis in stylized models of financial markets [40,41]. The results below do not change qualitatively for more general nonlinear impact functions [42].

To apply our model to the financial markets, we use the coupling strength k instead of D as the control parameter. Rather than assuming a fixed coupling strength for investors, we propose that the impact of colleagues' opinions on a given investor may be slowly varying with time. This effect reflects the fact that, in times of greater uncertainty, investors tend to be more influenceable by their surrounding [43]. There are many varying sources of uncertainty that impact financial markets, including the economic and geopolitical climate and past stock market performance. In the spirit of Ref. [44], all these factors are embodied into the notion that $K(t)$ undergoes a slow random walk with i.i.d. increments $K(t+\delta t) - K(t) \sim N(0, \sigma_k)$, which is confined in the interval $[k - \Delta k; k + \Delta k]$. This later constraint ensures that social imitation remains bounded. We could have used an Ornstein-Uhlenbeck process or any other such confining dynamics, without changing the crucial results presented below. More complex models of sophisticated investors involve the strategic adaptations of the traders' propensity to imitate to the reliability of their colleagues in recent outcomes [45–47].

By the mechanism of sweeping of the coupling strength $K(t)$ close to the critical coupling strength k_c (for fixed noise strength D) [48,49], we expect and find a transient burst of volatility in response to the aperiodic driving force $f(t)$ with constant amplitude and time scale. Figure 7 shows a typical realization, where the return $r(t)$ exhibits transient bursts,

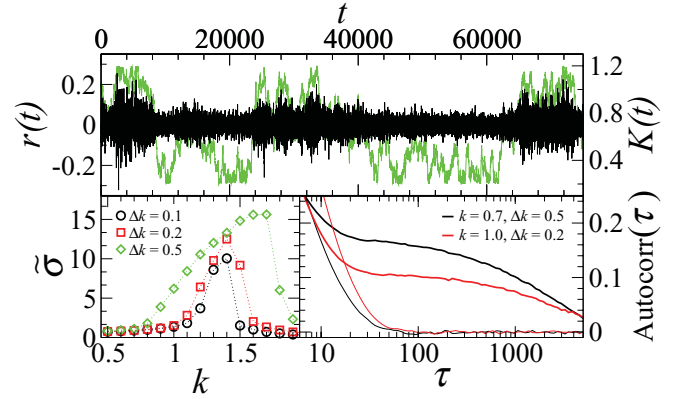


FIG. 7. (Color online) (Upper panel) Sample dynamics $r(t)$ (black bursty line) when the coupling strength $K(t)$ of the interactions between agents undergoes a confined random walk (green) in $[k - \Delta k; k + \Delta k]$ with $\Delta k = 0.5$ and step size $\sigma_k = \Delta k/\sqrt{5000}$. (Lower right panel) Quickly vanishing (respectively, long memory of) the autocorrelation of $r(t)$ (thin lines) [respectively, $|r(t)|$ (thick line)] for two values of k and of Δk . (Lower left panel) NIV resonance in the presence of a time varying $K(t)$, with $\Delta k = 0.1$ (circles), 0.2 (squares), 0.5 (diamonds). The other parameters are $N = 10^4$, $\sigma_{ap} = 0.04$, $D = 1$.

associated with excursion of $K(t)$ in the neighborhood of k_c . The lower left panel of Fig. 7 shows the robustness of the NIV phenomenon as a function of the average coupling k : Even with a fluctuating $K(t)$, a large volatility peak appears for intermediate values of k . The lower right panel shows very short-range correlations of $r(t)$ but very long-range correlations of the financial volatility $|r(t)|$ (another equivalent proxy for volatility), very similar to empirical observations of financial returns [31]. Such long persistence of the volatility can be traced back to the slow diffusive nature of $K(t)$ in line with the investors' slowly changing trust in the economy. From the previous section, it also follows that during times of crisis and strong social interaction (k close to k_c), the dynamics is generated mostly exogenously, well in line with the documented inability of news events to explain large price movements [30].

VI. CONCLUSIONS

In this paper, we have investigated the behavior of a system composed of coupled bistable units under the influence of a—rapidly varying—common exogenous forcing and independent noise sources. Independently of the shape of the driving force, intermediate noise strengths trigger a strong level of fluctuations of the macroscopic dynamics around the critical value separating the ordered from the disordered phases. For a periodic forcing, this peak corresponds to a pronounced amplification of the signal, with a strong correlation between the macroscopic dynamics and the driving force at the optimal lag, the paradigmatic signatures of stochastic resonance.

When the driving force is aperiodic a similar peak appears, but here the amplitude of the fluctuations exceeds by far those observed for periodic signals. Coincidental with the increase of fluctuations, the correlation between the driving force and the system dynamics is completely destroyed. This shows that

even though these fluctuations are induced by the common forcing, the macroscopic dynamics has an endogenous origin. This phenomenon of *noise-induced volatility* contrasts with that of stochastic resonance, with the major difference being that it is not the signal, but the fluctuations that are amplified.

Moreover, this phenomenon of *noise-induced volatility* also constitutes a new indicator for the approaching of a phase transition [32], and it applies to a broader range of real-world systems due to the more common setup given of a coupled system driving by an aperiodic forcing and its robustness with respect to changes in the underlying network of interactions.

As an example of a system where this phenomenon can be observed, we have proposed the social system of stock markets, in which we have been able to not only explain the excess of volatility observed in stock prices, but also the apparent absence of correlation between news and price changes and the persistence of volatility during times of crises.

APPENDIX: EQUIVALENCE TO THE KINETIC ISING MODEL WITH GLAUBER DYNAMICS

A popular update mechanism in the kinetic Ising model literature was introduced by Glauber [50]. In it, the probability for a spin to flip is given by

$$p_{\text{flip}} = \frac{1}{e^{\beta \Delta E_i} + 1}, \quad (\text{A1})$$

where ΔE_i is the energy gained by the system through the spin-flip and $\beta = 1/kT$. With $s_i = \pm 1$ and $E_i = -s_i(\sum_j K_{ij}s_j + f)$, which is the energy of the state s_i , Eq. (A1) can be rewritten as

$$p_{\text{flip}} = p_{s_i \rightarrow -s_i} = \frac{1}{e^{s_i 2\beta[\sum_j K_{ij}s_j + f(t)]} + 1} = \frac{1}{e^{s_i 2\beta\Lambda} + 1}, \quad (\text{A2})$$

where $\Lambda = \sum_j K_{ij}s_j + f$. With the transition rate given by Eq. (A2), we can compute the probability of being in state s_i

at time $t + \delta$ by

$$p(s_i; t + \delta) = p(s_i; t)p_{s_i \rightarrow s_i} + p(-s_i; t)p_{-s_i \rightarrow s_i} \quad (\text{A3})$$

$$\begin{aligned} &= p(s_i; t) \left(1 - \frac{1}{e^{s_i 2\beta\Lambda} + 1} \right) + p(-s_i; t) \frac{1}{e^{-s_i 2\beta\Lambda} + 1} \\ &= [p(s_i; t) + p(-s_i; t)] \frac{1}{e^{-s_i 2\beta\Lambda} + 1} \\ &= \frac{1}{e^{-s_i 2\beta\Lambda} + 1} = p(s_i), \end{aligned} \quad (\text{A4})$$

which is independent of time and gives us the probability of finding spin i in state s_i . Equation (A4) can be rewritten as

$$\begin{aligned} s_i(t + \delta) &= \begin{cases} +1 & \text{with Prob} = (e^{-2\beta\Lambda} + 1)^{-1} \\ -1 & \text{with Prob} = (e^{2\beta\Lambda} + 1)^{-1} \end{cases} \\ &= \begin{cases} +1 & \text{with Prob} = 1 - F(-\Lambda) \\ -1 & \text{with Prob} = F(-\Lambda), \end{cases} \end{aligned} \quad (\text{A5})$$

where $F(x)$ is the cumulative density function (CDF) of a logistic distribution with zero mean and variance $\pi^2/12\beta^2$.

The model studied in this paper, defined by Eq. (1), can be rewritten as

$$\begin{aligned} s_i(t + \delta) &= \begin{cases} +1 & \text{if } \xi_i(t) \geq -\Lambda \\ -1 & \text{if } \xi_i(t) < -\Lambda \end{cases} \\ &= \begin{cases} +1 & \text{with Prob} = 1 - G(-\Lambda) \\ -1 & \text{with Prob} = G(-\Lambda), \end{cases} \end{aligned} \quad (\text{A6})$$

with $G(x)$ being the CDF of the probability density function of $\xi_i(t)$, with zero mean and variance D^2 . By direct comparison of Eqs. (A5) and (A6), one can see that the model defined by Eq. (1) is equivalent to the kinetic Ising model with Glauber dynamics if the distribution of the noise is chosen to be a logistic distribution.

-
- [1] L. Gammaitoni, P. Hänggi, P. Jung, and F. Marchesoni, *Rev. Mod. Phys.* **70**, 223 (1998).
- [2] A. S. Pikovsky and J. Kurths, *Phys. Rev. Lett.* **78**, 775 (1997).
- [3] C. Van den Broeck, J. M. R. Parrondo, and R. Toral, *Phys. Rev. Lett.* **73**, 3395 (1994).
- [4] P. Hänggi and F. Marchesoni, *Rev. Mod. Phys.* **81**, 387 (2009).
- [5] D. Abbott, *Fluctuation and Noise Letters* **9**, 129 (2010).
- [6] B. McNamara, K. Wiesenfeld, and R. Roy, *Phys. Rev. Lett.* **60**, 2626 (1988).
- [7] K. T. Leung and Z. Néda, *Phys. Lett. A* **246**, 505 (1998).
- [8] K. T. Leung and Z. Néda, *Phys. Rev. E* **59**, 2730 (1999).
- [9] C. Nicolis, *J. Stat. Phys.* **70**, 3 (1993).
- [10] R. Benzi, G. Parisi, A. Sutera, and A. Vulpiani, *SIAM J Appl. Math.* **43**, 565 (1983).
- [11] J. K. Douglass, L. Wilkens, E. Pantazelou, and F. Moss, *Nature (London)* **365**, 337 (1993).
- [12] J. E. Levin and J. P. Miller, *Nature (London)* **380**, 165 (1996).
- [13] E. Simonotto, M. Riani, C. Seife, M. Roberts, J. Twitty, and F. Moss, *Phys. Rev. Lett.* **78**, 1186 (1997).
- [14] L. Gammaitoni, F. Marchesoni, and S. Santucci, *Phys. Rev. Lett.* **74**, 1052 (1995).
- [15] M. Acharyya, *International Journal of Modern Physics C* **16**, 1631 (2005).
- [16] G. Korniss, P. A. Rikvold, and M. A. Novotny, *Phys. Rev. E* **66**, 056127 (2002).
- [17] T. Tomé and M. J. de Oliveira, *Phys. Rev. A* **41**, 4251 (1990).
- [18] G. M. Buendía and P. A. Rikvold, *Phys. Rev. E* **78**, 051108 (2008).
- [19] S. W. Sides, P. A. Rikvold, and M. A. Novotny, *Phys. Rev. Lett.* **81**, 834 (1998).
- [20] J. J. Brey and A. Prados, *Phys. Lett. A* **216**, 240 (1996).
- [21] P. Jung, U. Behn, E. Pantazelou, and F. Moss, *Phys. Rev. A* **46**, R1709 (1992).
- [22] S. Ciliberto, *Physica D: Nonlinear Phenomena* **158**, 83 (2001).
- [23] M. C. Cross and P. C. Hohenberg, *Rev. Mod. Phys.* **65**, 851 (1993).
- [24] I. K. Ono, C. S. O'Hern, D. J. Durian, S. A. Langer, A. J. Liu, and S. R. Nagel, *Phys. Rev. Lett.* **89**, 095703 (2002).
- [25] R. B. Pandey and D. Stauffer, *J. Stat. Phys.* **61**, 235 (1990).
- [26] S. Bewick, R. Yang, and M. Zhang, *PLoS ONE* **4**, e8112 (2009).
- [27] D. Sornette, V. I. Yukalov, E. P. Yukalova, J. Y. Henry, D. Schwab, and J. P. Cobb, *J. Biol. Syst.* **17**, 225 (2009).
- [28] R. J. Shiller, *The American Economic Review* **71**, 421 (1981).

- [29] R. Brealey, S. Myers, and A. Marcus, *Fundamentals of Corporate Finance*, 6th ed. (McGraw-Hill Irwin, New York, 2009).
- [30] D. M. Cutler, J. M. Poterba, and L. H. Summers, *What Moves Stock Prices?* Tech. Rep. 2538 (National Bureau of Economic Research, 1989).
- [31] Z. Ding, C. W. J. Granger, and R. F. Engle, *Journal of Empirical Finance* **1**, 83 (1993).
- [32] M. Scheffer, J. Bascompte, W. A. Brock, V. Brovkin, S. R. Carpenter, V. Dakos, H. Held, E. H. van Nes, M. Rietkerk, and G. Sugihara, *Nature (London)* **461**, 53 (2009).
- [33] E. Stoll, K. Binder, and T. Schneider, *Phys. Rev. B* **8**, 3266 (1973).
- [34] K. Binder, *Rep. Prog. Phys.* **60**, 487 (1997).
- [35] M. E. J. Newman and G. T. Barkema, *Monte Carlo Methods in Statistical Physics* (Oxford University Press, New York, 1999).
- [36] P. Jung and P. Hänggi, *Phys. Rev. A* **44**, 8032 (1991).
- [37] S. J. Cornell, *Nonequilibrium Statistical Mechanics in One Dimension*, Cambridge Lecture Notes in Physics, Chap. 6 (Cambridge University Press, Cambridge, 1997), pp. 111–139.
- [38] W. Zwerger, *Phys. Lett. A* **84**, 269 (1981).
- [39] W. A. Brock and S. N. Durlauf, *The Review of Economic Studies* **68**, 235 (2001).
- [40] A. Beja and M. B. Goldman, *The Journal of Finance* **35**, 235 (1980).
- [41] M. Wyart and J.-P. Bouchaud, *J. Econ. Behav. Organ.* **63**, 1 (2007).
- [42] F. Lillo, J. D. Farmer, and R. N. Mantegna, *Nature (London)* **421**, 129 (2003).
- [43] S. Bikhchandani, D. Hirshleifer, and I. Welch, *The Journal of Political Economy* **100**, 992 (1992).
- [44] D. Stauffer and D. Sornette, *Physica A: Statistical Mechanics and its Applications* **271**, 496 (1999).
- [45] D. Sornette and W.-X. Zhou, *Physica A: Statistical Mechanics and its Applications* **370**, 704 (2006).
- [46] W. X. Zhou and D. Sornette, *The European Physical Journal B—Condensed Matter and Complex Systems* **55**, 175 (2007).
- [47] G. Harras and D. Sornette, *J. Econ. Behav. Organ.* **80**, 137 (2011).
- [48] D. Sornette, *Phys. Rev. Lett.* **72**, 2306 (1994).
- [49] D. Sornette, *J. Phys. I* **4**, 209 (1994).
- [50] R. J. Glauber, *J. Math. Phys.* **4**, 294 (1963).